THE JOURNAL OF COMPARATIVE NEUROLOGY 410:143–157 (1999)

Increased Corticofugal Plasticity After Unilateral Cortical Lesions Combined With Neutralization of the IN-1 Antigen in Adult Rats

CHRISTIAN A. WENK, MICHAELA THALLMAIR,* GWENDOLYN L. KARTJE, AND MARTIN E. SCHWAB
Brain Research Institute, University of Zurich and Swiss Federal Institute of Technology Zurich, CH-8057 Zurich, Switzerland

ABSTRACT

If damage to the central nervous system (CNS) occurs early in life, extensive rearrangements of the remaining fiber systems as well as regeneration of lesioned fibers take place. In the rat or hamster, newly grown projections have been described only if the lesion occurred within the first two weeks postnatally. This decreasing growth ability correlates with CNS maturation and the progression of myelination. Myelin contains the potent neurite growth inhibitors NI-35/250 that are crucially involved in the failure of long-distance regeneration and the lack of compensatory structural plasticity after adult CNS lesions. In this study, we show that extensive remodeling occurs well after the termination of the growth permissive period in the adult rat if we neutralize the inhibitory properties of myelin with the monoclonal antibody IN-1. After ablation of one motor cortex and treatment with the antibody IN-1, we observed that the remaining corticospinal tract (CST) from the spared hemisphere sprouted into the denervated, contralateral red nucleus and pons. In the pons, these fibers terminated in a typical somatotopic pattern. For comparison with neonatal plasticity, we performed the same lesion in two-day-old rats (no antibody). This lesion led as well to sprouting of the remaining CST into denervated brainstem nuclei, resulting in a bilateral corticofugal projection. Our results show that neutralization of myelin-associated neurite-growth inhibitors after CNS lesions leads to a structural remodeling of the spared corticofugal fibers in adult rats, a process normally restricted to a short postnatal period. J. Comp. Neurol. 410:143–157, 1999.

Indexing terms: sprouting; CNS myelin; motor system; critical period; red nucleus; pons

Brain damage early in life evokes a variety of plastic changes within the central nervous system (CNS); these can lead to new neuronal connections that might differ from the normal developmental pattern (Kuang and Kalil, 1990; for review, see Kolb and Whishaw, 1989). A high degree of functional recovery is usually seen after these neonatal CNS lesions (Whishaw and Kolb, 1988; Barth and Stanfield, 1990). In the case of unilateral cortical damage, the formation of an "aberrant" ipsilateral corticospinal tract (CST) from the spared hemisphere was described that might be the anatomical correlate for the sparing of skilled forelimb reaching (Hicks and D'Amato, 1970; Leong and Lund, 1973; Castro, 1975; Leong, 1976; Kartje-Tillotson et al., 1985, 1987; Gomez-Pinilla et al., 1986; Whishaw and Kolb, 1988; Barth and Stanfield, 1990; Kuang and Kalil, 1990). Additionally, an increased crossed projection from the intact hemisphere to the contralateral basilar pontine nuclei, red nucleus, and striatum have been described (Leong and Lund, 1973; Nah and Leong, 1976; Mihailoff and Castro, 1981; Villablanca et al., 1982; Kartje-Tillotson et al., 1986; Murakami and Higashi, 1988;

Grant sponsor: Swiss National Science Foundation; Grant numbers: 31–45549.95 and 4038–43918.95; Grant sponsors: the Biotechnology Program of the European Union, Brussels; the Dr. Eric Slack-Gyr-Foundation, Zurich; the American Paralysis Association, Springfield, NJ; the International Research Institute for Paraplegia, Zurich; and the Binelli-Ehrsam-Foundation, Zurich.

Gwendolyn L. Kartje's present address: Neurology Service, Edward Hines Jr. Veterans Affairs Hospital, Hines, IL, 60141 and Departments of Neurology and Cell Biology, Neurobiology, and Anatomy, Loyola University, Maywood, IL, 60153.

*Correspondence to: Michaela Thallmair, Brain Research Institute, University of Zurich and Swiss Federal Institute of Technology Zurich, Winterthurerstr. 190, CH-8057 Zurich, Switzerland.
E-mail: thallm@hifo.unizh.ch

Received 19 November 1998; Revised 1 February 1999; Accepted 22 February 1999

Kolb et al., 1992). In contrast to the flexible "rewiring" and functional recovery after lesions in the immature CNS, functional and anatomical repair is very limited in the adult brain and spinal cord (Kennard, 1936, 1938; Kuang and Kalil, 1990). Interestingly, the decrease of lesion-induced sprouting within the first two weeks postnatally correlates in time and location with the progression of myelination in white and gray matter (Kapfhammer and Schwab, 1994). Myelin contains factors that may contribute to the termination of the growth-permissive period, the myelin-associated neurite growth inhibitors NI-35 and NI-250. These proteins induce long-lasting growth cone collapse and inhibit neurite growth in vitro (Caroni and Schwab, 1988a; Bandtlow et al., 1990; Spillmann et al., 1998). The monoclonal antibody IN-1 that was raised against these inhibitory proteins allowed neurite outgrowth on CNS myelin or cultured oligodendrocytes in vitro (Caroni and Schwab, 1988b). In vivo application of mAb IN-1 led to long-distance regeneration after CST lesions in adult rats (Schnell and Schwab, 1990, 1993; Schnell et al., 1994) and to functional recovery of some locomotor functions (Bregman et al., 1995). In addition, neutralization of the myelin-associated neurite growth inhibitors allows compensatory structural plasticity and restoration of function in response to an adult focal CST lesion (Thallmair et al., 1998; Z'Graggen et al., 1998).

In the present study, we examined remodeling of the corticorubral and corticopontine projections from the spared hemisphere in adult rats after a unilateral motor cortex ablation and mAb IN-1 treatment. To compare these results with the structural plasticity seen after neonatal cortical ablations, a group of rats underwent cortical lesion at two days of age. The anterograde tracer biotin dextran amine (BDA) (Brandt and Apkarian, 1992; Veenman et al., 1992) was used to trace the projections of the intact forelimb motor area to the red nucleus and the basilar pontine nuclei in all animal groups. Our results show topographically specific structural plasticity comparable to that seen after neonatal lesions in the red nucleus and the basilar pontine nuclei following unilateral lesions of the caudal motor cortex in adult, mAb IN-1-treated rats.

MATERIALS AND METHODS

All animal experiments were carried out under the supervision of the veterinary department of the Canton of Zurich, Switzerland. Institutional guidelines for animal care and safety were adhered to. Animals were housed in groups and had free access to food and drinking water. Figure 1 illustrates the experimental procedures.

Animals

The study was performed on 35 male Lewis rats from our own breeding colony. Twenty-four animals underwent a unilateral aspiration lesion of the caudal motor cortex at an age of 50–55 days. Six animals of the same age served in the anatomy control group, and five animals underwent cortical lesion at postnatal day 2 (P2). BDA was injected into the intact forelimb motor cortex of all rats (see next section for details). The animals were divided into the following five groups:

Unlesioned, untreated animals (n = 6; anatomy)
Adult cortical lesion (n = 6) without further treatment (lesion only)
Adult cortical lesion (n = 8) receiving a treatment with a control antibody against horseradish peroxidase (anti-HRP)
Adult cortical lesion (n = 10) receiving a treatment with the monoclonal antibody against the myelin-associated neurite growth inhibitor (mAb IN-1)
Neonatal lesioned animals (n = 5) without any further treatment used for comparison with the adult lesioned mAb IN-1-treated animals (P2-lesion)

Surgery of adult rats: Tracing, lesion, and tumor application

The animals were pretreated with atropine (0.025 mg, i.p., Sintetica, Mendrisio, Switzerland) and anesthetized with ketamine (Ketalar, Parke- Davis, Morris Plains, NJ; i.p., initial dose 100 mg/kg body weight followed by supplemental doses of 40 mg/kg injected i.m. whenever necessary depending on the reflex status of the animal). The animals were placed in a stereotaxic frame, lying on a heating pad (37°C), allowing the forelimbs to hang free for a better observation of movements during intracortical microstimulation (ICMS). The skull was exposed with a midline skin incision, and the bone overlying the right caudal motor cortex area was removed (stereotaxic coordinates: 1–4 mm lateral; 2.5 mm rostral to 1 mm caudal relative to Bregma). The craniotomy was made without damaging the dura, and the brain was protected with mineral oil. The cisterna magna was opened and drained to reduce swelling of the cortex.

For ICMS, five points in the caudal forelimb motor cortex were chosen corresponding to the map of Neafsey et

Abbreviations

3.V	third ventricle
ABC	avidin-biotin complex
BDA	biotinylated dextran amine
BSA	bovine serum albumin
Cc	corpus callosum
CCD	charge-coupled device
cer. ped.	cerebral peduncle
CNS	central nervous system
Cp	cerebral peduncle
CST	corticospinal tract
DAB	3,3′ diaminobenzidine tetrahydrochloride
ELISA	enzyme-linked immunosorbent assay
FITC	fluorescein isothiocyanate
GAP-43	growth-associated protein 43
Hi	hippocampus
HRP	horseradish peroxidase
ICMS	intracortical microstimulation
IN-1	inhibitor neutralizing protein 1
iOD	integrated optical density
i.m.	intramuscular
i.p.	intraperitoneal
l.V	lateral ventricle
mAb	monoclonal antibody
MCID	microcomputer imaging device
N	number of animals
NI	neurite inhibitor
OD	optical density
P2	postnatal day 2
P3U	mouse myeloma cell line (P3X63Ag8U.1)
R	regression coefficient
SEM	standard error of the mean
T	tumor
TBST-X	Tris-buffered saline solution with Triton X-100

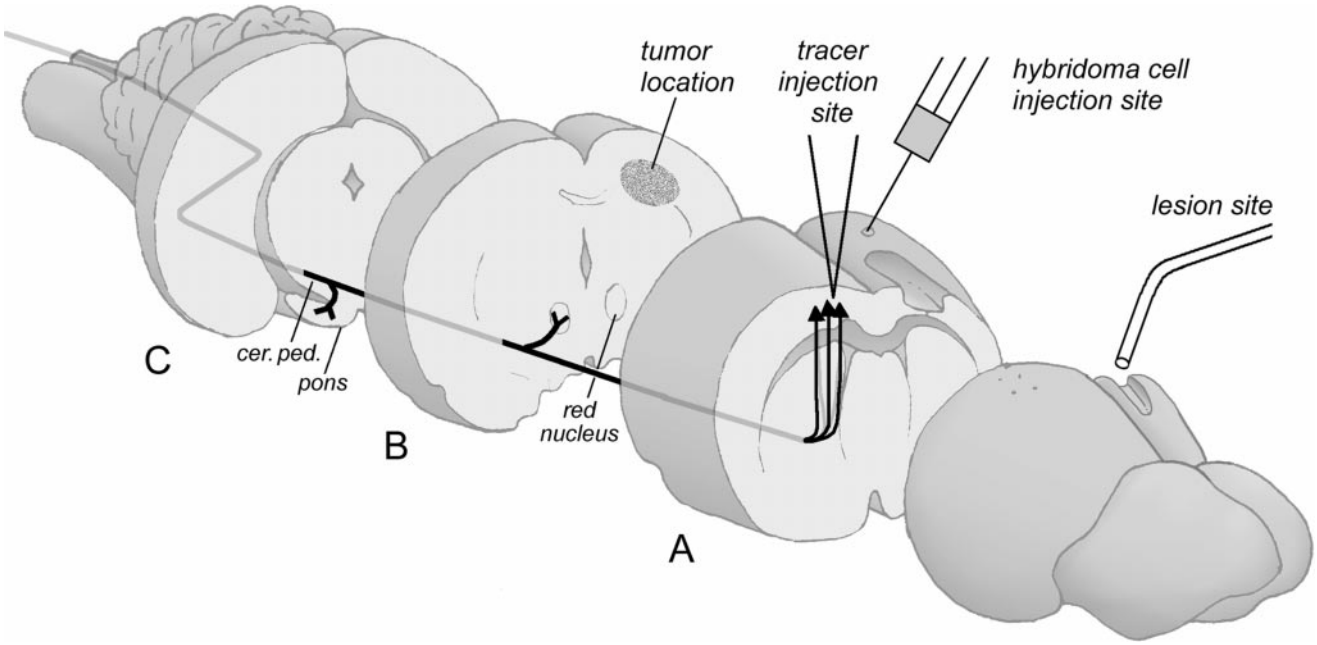

Fig. 1. Schematic illustration of the experimental procedures. Corticofugal fibers from the right forelimb motor cortex to the termination areas in the red nucleus and in the basilar pontine nuclei are represented. Cross sections: **A**, BDA injection region; **B**, at the level of the red nucleus; and **C**, at the level of the cerebral peduncle and the basilar pontine nuclei. In the left hemisphere are schematically shown the aspiration lesion, the hybridoma cell implantation site, and the location of the tumor. The BDA tracer injection sites are contralateral to the lesion.

al. (1986): 2 mm lateral, 0 mm rostral; 2.5 mm lateral, 0.5 mm rostral; 3 mm lateral, 0.5 mm rostral; 2.5 mm lateral, 1 mm rostral; 3 mm lateral, 1 mm rostral relative to Bregma. Using a thin low-impedance tungsten microelectrode, forelimb movements were evoked with low currents (to prevent cortical damage, the maximum current was 20 µA), 60 ms train, 0.2 ms cathodal pulses, 330 Hz at a depth of 1.7–1.9 mm. A point was accepted for iontophoresis of the BDA tracer when the threshold for forelimb movement stimulation was lower than 14 µA. Higher thresholds or blood vessels on the cortex surface caused in some cases a small shift of the coordinates.

For iontophoresis, the lesion, and the hybridoma-cell implantation, ketamine treatment was stopped and a single dose of midazolam (4 mg/kg body weight, Dormicum, Roche, Basel, Switzerland) was injected intraperitoneally. To visualize the projection originating in the caudal forelimb area, 10% BDA (10 kD MW, Molecular Probes, Eugene, OR) in phosphate buffer (10 mM, pH 7.2) was iontophoretically injected (Graybiel and Devor, 1974): a glass micropipette (tip-diameter 20 µm) was inserted perpendicular to the surface of the cortex at the five points determined by microstimulation, and BDA was injected iontophoretically at the depth of lowest threshold (5 µA, pulse duration 7 seconds, interval 14 seconds) for 15 minutes at each point. The cortex was then covered with Gelfoam and the skull closed with dental cement. The skin of the anatomy animals was sutured, whereas all the other animals underwent a unilateral aspiration lesion of the contralateral, left caudal motor cortex. For that reason, a second craniotomy was made and the dura was removed using forceps and a scalpel blade. The exposed cortex was aspirated with a small glass pipette to a depth of 2 mm (1–5 mm lateral and 3 mm rostral to 3.5 mm caudal relative to Bregma).

In the two groups (n = 18) receiving a hybridoma-cell implantation a small craniotomy 3 mm lateral and 5 mm caudal to Bregma was made with the dental drill and 6 µl of a cell suspension containing a total number of 10^5 living hybridoma cells was slowly injected into the lesioned hemisphere at a depth of 3 mm using a 10 µl Hamilton syringe (Schnell and Schwab, 1990; Thallmair et al., 1998). One group (n = 10) received cells secreting the monoclonal antibody IN-1 against the rat neurite growth inhibitory protein NI-250 (Caroni and Schwab, 1988b), and the other group (n = 8) received control cells producing an antibody against horseradish peroxidase (anti-HRP) generated from the same parent myeloma cell line P3U (Schnell and Schwab, 1990). Cultured hybridoma cells were regularly checked for their IN-1 or anti-HRP antibody production before they were implanted. The skin was sutured, and the animals were returned to their cages after giving another dose of midazolam (2 mg/kg, i.p.). The day before the surgery and during the entire survival period of 14 days, the animals received a daily injection of cyclosporin A (10 mg/kg body weight, i.p., Sandimmun, Novartis, Basel, Switzerland) to prevent an immune reaction against the implanted cells. The non-lesioned and lesion only animals received the same cyclosporin treatment. An antibiotic treatment with co-trimoxazol (0.83 mg/kg body weight, i.p., Bactrim, Roche, Basel, Switzerland) was started at the same time in all animals.

After the survival period of 14 days, all animals were killed by an overdose of pentobarbital (450 mg/kg body weight, i.p., Nembutal, Abbott Laboratories, Cham, Switzerland) and perfused through the heart with a Ringer's

solution containing 20,000 U/l heparin (Liquemin, Roche, Basel, Switzerland) and 0.25% $NaNO_2$ followed by the fixative of 4% paraformaldehyde in 0.1 M phosphate buffer and 5% sucrose. The brains were removed and postfixed in 4% paraformaldehyde for one day before being immersed in 30% sucrose at 4%C for cryoprotection.

Neonatal surgery

Pups at two days of age (P2) were anesthetized by hypothermia. The cranium was exposed with a midline skin incision, and the skull overlying the left frontal cortex was removed with forceps. The dura was opened using small forceps and a scalpel blade, and the sensorimotor cortex was aspirated by mild suction with a small glass pipette as previously described (Kartje-Tillotson et al., 1985). The wound was packed with gelfoam and the skin sutured. The pups were warmed under an incandescent lamp, returned to their mothers until weaning, and then housed together until they were one year old. The ICMS and iontophoresis procedures were performed as described for the adult lesioned animals with the exception that in these animals the caudal forelimb motor cortex of the intact side and consequently the tracer injection points were shifted rostrally as a result of the neonatal lesion (Papathanasiou et al., personal communication). The survival time after iontophoretic BDA injection was 14 days.

Tissue processing

After immersion in sucrose for three days, the brains were cut into two parts at the level of the thalamus. The brainstem was separated from the spinal cord just caudal to the CST decussation. The dura was carefully taken off, and the cerebellum was removed. Then the tissue was embedded in gelatin-chicken albumin solution polymerized with 25% glutaraldehyde (Herzog and Brösamle, 1997) and immediately frozen by immersion in −40°C isopentane. Cross sections of 50 µm were cut on a freezing microtome. Every second section of the brain and each section of the brainstem were serially mounted on Superfrost slides (Menzel-Gläser, Germany) and reacted for BDA using the semifree-floating method (Herzog and Brösamle, 1997). Briefly, the slides were washed three times for 30 minutes in 50 mM Tris-buffered saline (0.9%, pH 8.0) with 0.5% Triton X-100 (TBST-X) and incubated over night at 4°C with an avidin-biotin-peroxidase complex (ABC Elite, Vector, Burlingame, CA) diluted in TBST-X. The next day slides were washed again three times for 10 minutes in TBST-X, rinsed in 50 mM Tris-HCl buffer (pH 8.0), and preincubated in 0.4% nickel ammonium sulfate (Sigma, St. Louis, MO) in 50 mM Tris-HCl for 10 minutes. Sections were further preincubated for 10 minutes in the nickel ammonium sulfate solution to which 0.015% of 3,3′ diaminobenzidine tetrahydrochloride (DAB; Sigma, Buchs, Switzerland) was added and finally reacted in a nickel ammonium/DAB mixture containing 0.004% H_2O_2. After 10–20 minutes the reaction was stopped with 50 mM Tris-HCl and the sections were rinsed three times for 10 minutes in 50 mM Tris-HCl. Sections were air dried, dehydrated, and embedded in Eukitt (Kindler, Freiburg, Germany).

Neuroanatomical analysis

All anatomical structures were identified with help of the atlas of Paxinos and Watson (1982). The BDA injection site and the cortical lesion were analyzed for their localization, extent and depth (Fig. 3A,B). The hybridoma cell injection region was examined for the presence of the hybridoma xenografts. When an antibody-producing tumor—or necrotic tissue when the tumor was already resorbed—was found close to the hippocampal formation and the third ventricle (Fig. 3C), the brains were further analyzed. Brains that showed no signs of a tumor or brains showing enlarged tumor invasion to deeper regions resulting in a compression of brainstem structures were not included in the study.

In the brainstem, the red nucleus (parvocellular part) and the basilar pontine nuclei (dorsolateral, dorsomedial, lateral, intermedial, and medial pontine nucleus; Mihailoff et al., 1978), were qualitatively and quantitatively analyzed ipsi- and contralaterally to the injection site.

For the quantitative, densitometric analysis, electronic images were acquired with a Xillix Microimager slow-scan, high-resolution CCD camera attached to a Zeiss axiophot microscope. All analyses of these images were performed with the MCID-program (M2 Analyzing Program; Imaging Research, Ontario, Canada): we measured the optical density over an area A (integrated optical density = iOD), which represented a value for the number of labeled fibers contained in this area. To test for linearity of the iOD to the number of labeled fibers, measurements of the iOD and counts of labeled fibers (over the same area) were made for 11 regions of different fiber density in the cerebral peduncle (Fig. 2A) and in a pontine projection area (Fig. 2B). The results showed a linear, significant relationship with a very high correlation between iOD and actual fiber numbers in both regions (Fig. 2A,B).

Background corrections were done by subtracting the optical density (extrapolated to the area A) of surrounding tissue (containing no labeled fibers):

$$iOD = iOD_A - ((A/B) \times iOD_B)$$

where iOD = calculated integrated optical density (of labeled fibers only) in a projection area (A); iOD_A = measured integrated optical density over area A (inclusive background); B = area of surrounding tissue including no labeled fibers; and iOD_B = measured integrated optical density over area B (background only).

Quantification of CST labeling in the cerebral peduncle. The numbers of labeled CST axons in the cerebral peduncle were determined and used to normalize the inter-animal variations in the BDA tracing. The ipsilateral labeled cerebral peduncle on five consecutive sections of the intermediate part of the pons was measured (iOD_A), and the contralateral unlabeled cerebral peduncle served as iOD_B for background subtraction. The resulting iOD values and the calibration (iOD vs. number of labeled CST axons; Fig. 2A) were used to extrapolate the total number of labeled CST fibers (Fig. 2C). Statistical significance of differences of the labeled CST-axon numbers was assessed with the unpaired t-test assuming unequal variances.

Quantification of the corticorubral projection. The crossed corticorubral projection originating in the tracer-injected forelimb motor cortex contralateral to the lesion was analyzed by counting all BDA-positive fibers crossing the midline on 15 sections containing the parvocellular part of the red nucleus. In each animal the values of the 15 sections through the red nucleus were added up for the total number in each animal. To correct for the inter-animal tracing differences, the values were divided by the number of labeled CST fibers in the cerebral peduncle and expressed as fibers crossing the midline per 1,000 labeled

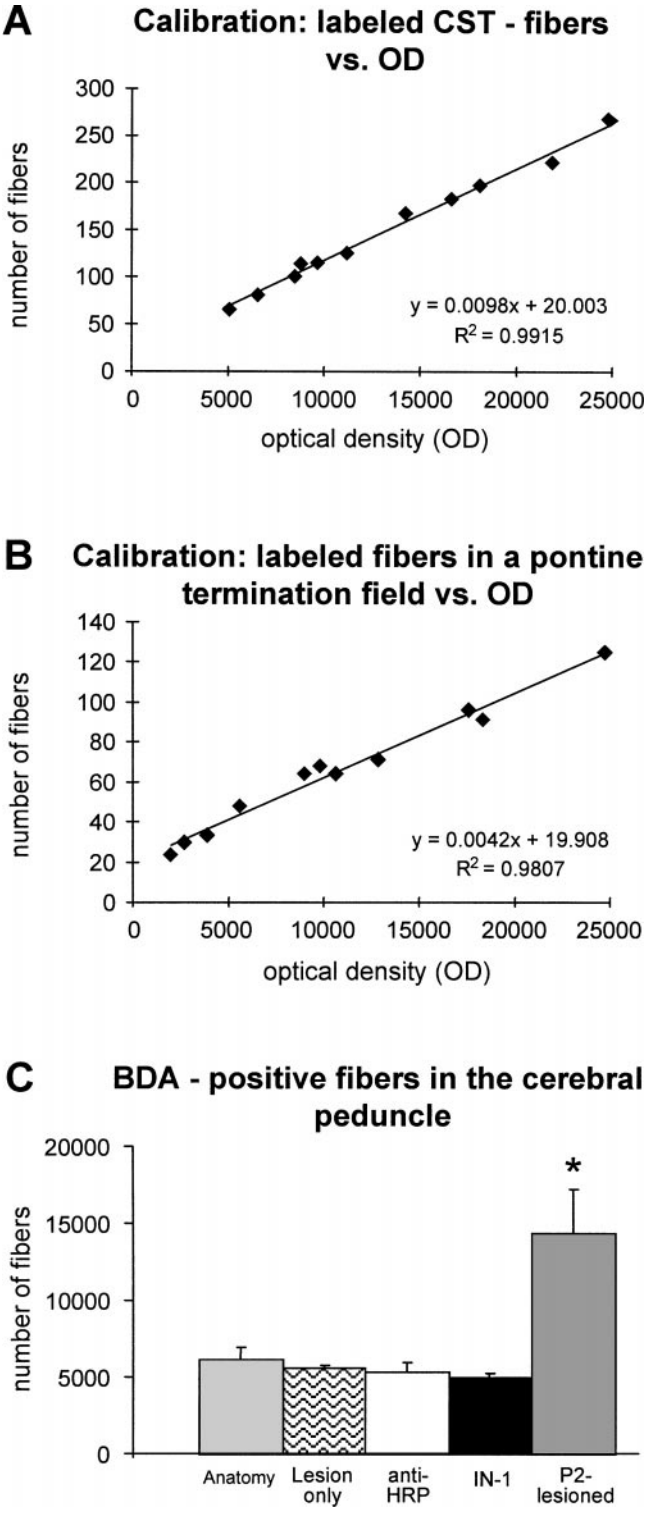

Fig. 2. Calibration and normalization of fiber density determinations. **A:** Linear relationship between the number of labeled CST-axons in the midpontine cerebral peduncle and their optical density. **B:** Same procedure as in A for fibers in a pontine termination field. **C:** Total number of labeled CST-axons in the cerebral peduncle at midpontine level. These numbers were used as normalization values for the inter-animal tracing differences. Significantly more CST fibers are found in neonatally lesioned animals. Mean values ± SEM. The asterisk indicates a significant difference between P2-lesioned and adult lesion only animals; $*P < 0.05$, t-test, two tailed.

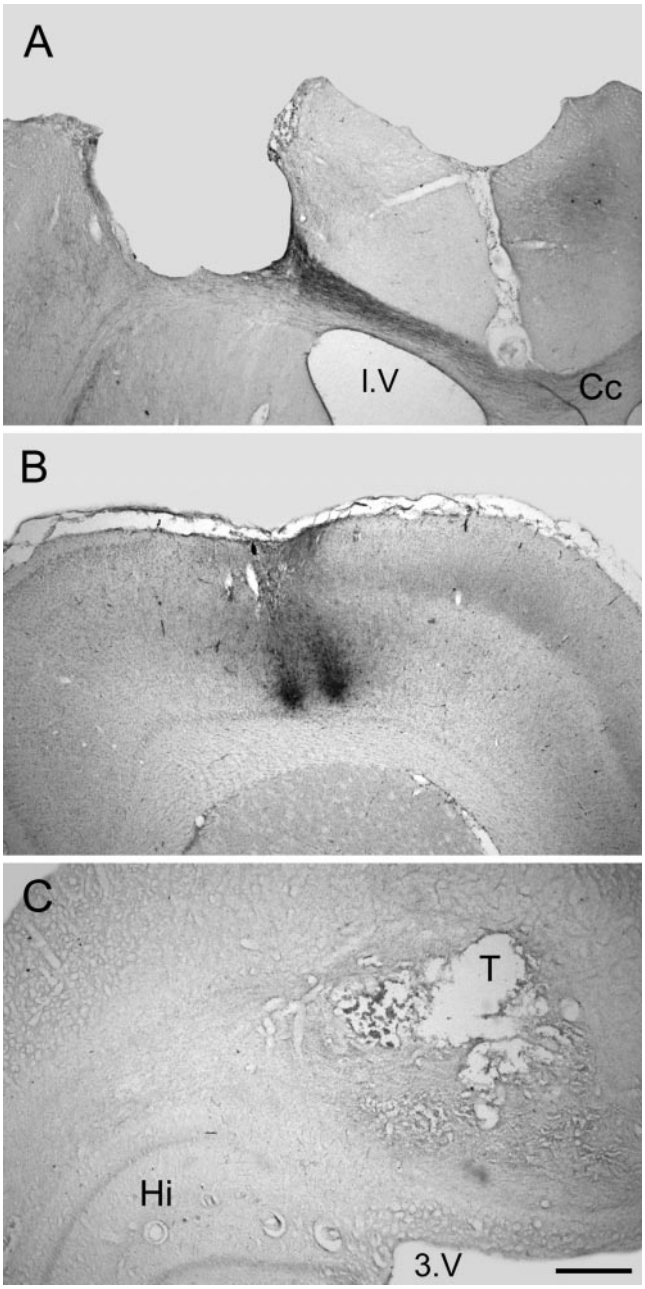

Fig. 3. Photographic illustrations of the experimental procedures. **A:** Photomicrograph of a cross section through a lesioned, rat motor cortex, 2 mm rostral to Bregma. **B:** Section through the intact hemisphere with two BDA tracer injection sites 0.5 mm rostral to Bregma. **C:** Tumor location close to the hippocampus and the third ventricle. Lesion and tumor are localized in the left and the tracer injection site in the right cortical hemisphere. Scale bar = 640 µm.

CST axons. Statistical significance was assessed using the unpaired t-test assuming unequal variances. The course and termination fields of fibers projecting to the red nucleus were qualitatively analyzed.

Quantification of the corticopontine projection. All sections comprising the pons (30–35 sections corresponding to a rostrocaudal distance of 1.5–1.75 mm) were included in the analysis. On each section, the labeling of

all basilar pontine nuclei ipsi- and contralaterally to the injection site was densitometrically determined, resulting in the iOD_A values. For background subtraction the optical density of unlabeled neighboring areas (iOD_B) was measured. The calculations of iOD were made as described above, separately for the ipsilateral and the contralateral side. The contralateral labeling was then expressed as a percentage of the ipsilateral innervation (ratio iOD contralateral/iOD ipsilateral). Furthermore, all pontine fibers crossing the midline were counted and normalized for inter-animal tracing differences, resulting in values expressing numbers of midline crossing fibers per 1,000 labeled axons in the CST. The contralateral innervation density of labeled fibers was further brought in relation to the number of midline crossing fibers (iOD of the contralateral side per midline crossing fiber). The innervation index given in Figures 6 and 7 represents the normalized iOD values.

For analysis of innervation specificity, the pons was divided into three parts:

Rostral part of the pons containing one forelimb-related projection field
Intermediate part showing five columns: dorsolateral, lateral, intermedial, medial and dorsomedial pontine nucleus (Mihailoff et al., 1978; Wiesendanger and Wiesendanger, 1982); in the analysis the values of the dorsolateral and lateral pontine nucleus and of the dorsomedial and the medial nucleus were combined
Caudal part with one large central projection area

The same analysis as described above for the entire pons was made separately for each part of the pons. As the values of the non-lesioned, the lesion only, and the anti-HRP-treated animals did not differ significantly, they were taken together into one control group and compared with the mAb IN-1-treated animals and with the neonatal lesioned animals, respectively (Figs. 6F, 7). Values for the rostral, intermedial, and caudal parts were expressed as a percentage of the values of the entire pons. Thus, the total of the three values of one group in Figures 6F and 7 always added up to 100%.

In addition to the analysis of the rostrocaudal fiber distribution, we also studied the mediolateral distribution of the corticopontine innervation. Electronic images were acquired with a Xillix CCD camera attached to a Zeiss axiophot microscope using a 4× objective. With the MCID-program the optical density (OD) was measured and integrated over a bar-shaped field (50 × 2300 µm) placed horizontally over the densest areas of the labeled projection on the sections, thus resulting in integrated optical density values (iOD). In the images, 500 pixels corresponded to a distance of about 900 µm on the sections (see Fig. 8).

Differences were tested for statistical significance between lesioned, mAb IN-1 and lesioned, anti-HRP-treated animals and between neonatally lesioned and lesion only animals (exceptions are mentioned in the figure legends) using the unpaired t-test (unequal variances).

Figure preparation

Electronic images were acquired with a Xillix Microimager slow-scan, high resolution CCD camera attached to a Zeiss axiophot microscope. Images were assembled in Photoshop 4.0 (Adobe). Contrast was adjusted, when necessary.

RESULTS

Lesion site and antibody application

Histological examination of all lesions in the left motor cortex showed that there were only small variations in the extent or placement of the lesion (maximum 0.5 mm shift from the reference lesion site; see Materials and Methods). All cortical layers of the motor cortex were removed without damaging subcortical structures. A representative lesion can be seen in Figure 3A.

Hybridoma cells were implanted close to the hippocampal region and the third ventricle ipsilateral to the lesion site (Fig. 3C). In some cases, the cells invaded the lesion site, or an increased cell division rate led to a contusion of neighboring brain areas. Animals with tumors of this extent were excluded from further analysis (n = 6). In vivo mAb secretion was tested by staining with FITC-labeled anti-mouse antibody in analogous experiments. A high level of mouse antibodies in the tumors, the ventricles, and the brain surfaces could be seen (data not shown; Schnell and Schwab, 1990). A weak staining could be detected in the parenchyma of the brainstem (Z'Graggen et al., 1998).

Tracing of the forelimb corticofugal axons

BDA injection sites showed most of the tracer localized in layer V (Fig. 3B) with only small amounts in other layers and without affecting the underlying white matter.

The distribution of BDA-positive fibers corresponding to the forelimb corticofugal pathway in cross sections of the cerebral peduncle was similar in all animal groups, except for the neonatally lesioned group. In the latter group the distribution of labeled fibers was homogenous across the entire cerebral peduncle, with only a slight decrease of labeling laterally. In all other groups, however, most BDA-positive fibers were found in the medial half of the peduncle, with only a minor portion situated more laterally (Mihailoff et al., 1978; Kosinski et al., 1986). The average numbers of BDA-labeled fibers in the cerebral peduncle at midpontine level were similar in the different adult treatment groups: 4998 (± 318 SEM, n = 10) in lesioned, mAb IN-1-treated animals, 5347 (± 675 SEM, n = 8) in lesioned, anti-HRP-treated animals, 5635 (± 179 SEM, n = 6) in animals with lesion only, and 6204 (± 780 SEM, n = 6) in normal, unlesioned animals (Fig. 2C). Interestingly, the neonatally lesioned animals showed a greatly increased number of fibers in the cerebral peduncle compared with the other groups: 14,384 (± 2886 SEM, n = 5, Fig. 2C).

Plasticity of the corticorubral projection

The ipsilateral corticorubral projection originating in the caudal cortical forelimb area showed a similar pattern in all animal groups. At midbrain levels the labeled fibers left the cerebral peduncle from its dorsal aspect, passed the substantia nigra, where some fibers terminated, and then turned sharply medial and dorsal, toward the red nucleus, projecting mainly to the parvocellular part (Fig. 4A) in a similar fashion as described by others (Fig. 4A; Brown, 1974; Flumerfelt, 1980; Naus et al., 1985a). In addition, a few fibers terminated in the magnocellular part (Z'Graggen et al., 1998). In normal animals, none or only a few BDA-labeled fibers crossed the midline and terminated in the contralateral red nucleus, primarily in the parvocellular region.

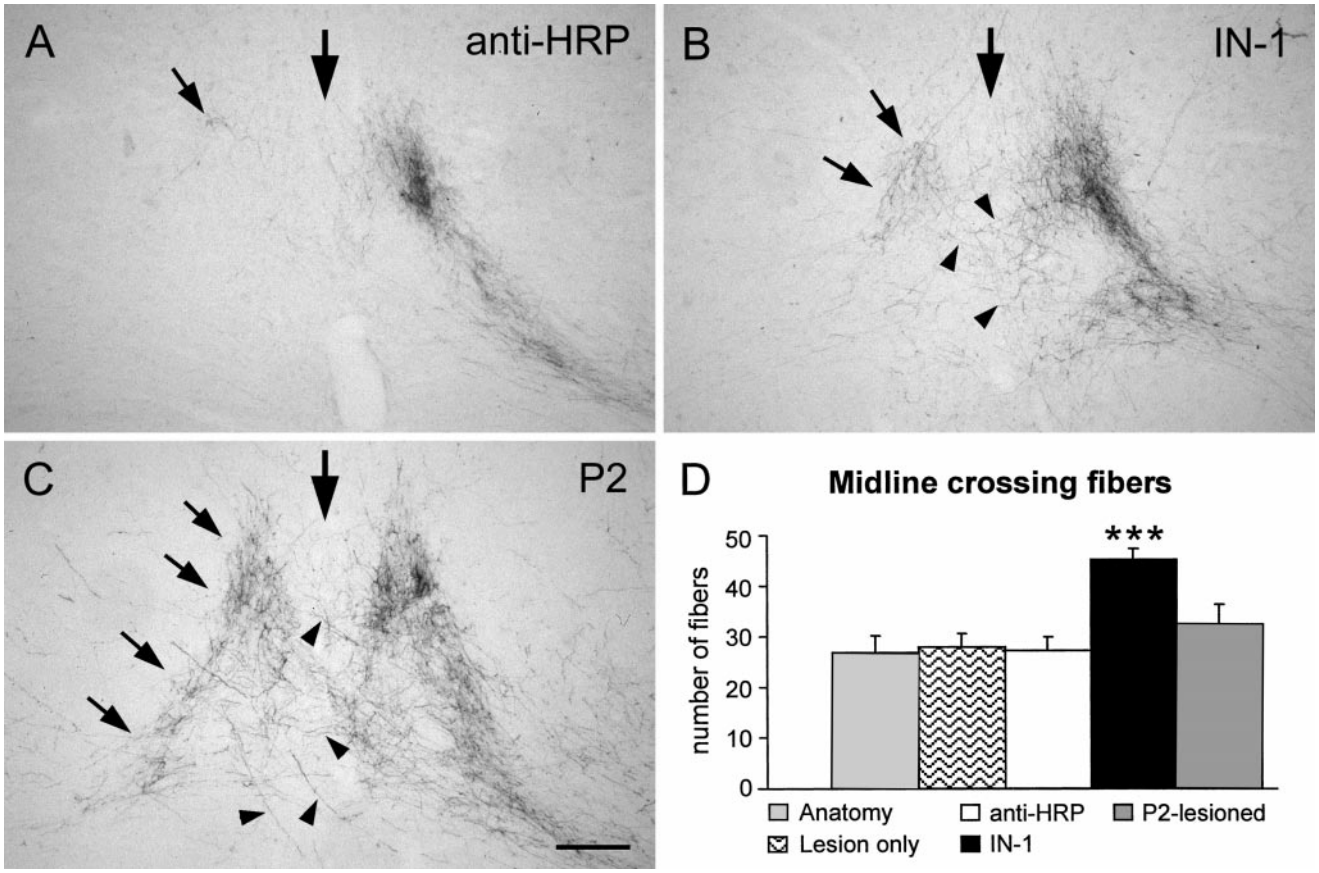

Fig. 4. Corticorubral projection; cross sections through the parvocellular red nucleus (A–C) and quantification of midline crossing fibers (D). In A–C, the large arrow shows the midline, the small arrows the contralateral projection, and the arrowheads the midline crossing fibers. **A:** Corticorubral projection after treatment with the control, anti-HRP antibody during 2 weeks (survival time after lesion). A very small termination area of labeled fibers crossing the midline (large arrow) to the denervated side (small arrow) is visible. **B:** Termination pattern in a mAb IN-1-treated animal. The photomicrograph shows many midline crossing fibers (arrowheads) and a denser innervation contralateral to the tracer injection compared with control rats. **C:** Neonatally lesioned animals show a very dense projection to the denervated side and, as in the mAb IN-1-treated animals, the contralateral termination pattern mirrors the ipsilateral one. **D:** Relative numbers of labeled fibers (per thousand labeled CST-axons) crossing the midline in the parvocellular red nucleus (15 sections). In mAb IN-1-treated animals significantly more corticorubral fibers per thousand labeled CST-axons cross the midline, whereas P2-lesioned animals show only a small increase. Error bars indicate mean values ± SEM. Asterisks indicate significance (IN-1 compared with anti-HRP); ***, $P < 0.001$, t-test, two tailed. Scale bar = 160 μm.

Rats with a unilateral cortical lesion without any antibody treatment, and lesioned anti-HRP-treated animals were indistinguishable from these normal animals (Fig. 4A). In lesioned, mAb IN-1-treated animals, the ipsilateral corticorubral projection was similar to the control groups, but significantly more BDA-positive fibers crossed the midline and terminated in the deafferented, contralateral red nucleus (Fig. 4B,D). Neonatally lesioned animals also showed an increase in midline-crossing fibers resulting in a very dense innervation of the contralateral, denervated red nucleus, where the fiber distribution precisely mirrored the ipsilateral projection (Fig. 4C). In the mAb IN-1-treated animals and in the P2 group, many fibers bypassed the ipsilateral parvocellular red nucleus ventrally to project directly to the corresponding contralateral area, some of them showing bouton-like endings. Other midline crossing fibers seemed to be branches of axons also terminating ipsilaterally or coursing through the ipsilateral parvocellular red nucleus to reach the contralateral parvocellular red nucleus.

Counting of the midline crossing fibers in the parvocellular region of 15 sections after correction for the interanimal tracing variations resulted in 26.75 ± 3.38 fibers per 1,000 labeled CST-axons in normal, 27.9 ± 2.75 fibers in lesion only, 27.35 ± 2.64 fibers in lesioned, anti-HRP-treated animals, and 45.24 ± 2.19 fibers in the lesioned, mAb IN-1-treated animals (Fig. 4D). The mAb IN-1 treatment in lesioned, adult rats thus resulted in a 1.7-fold increase of midline crossing fibers compared with the control groups. Neonatally lesioned animals showed 32.4 ± 4.01 labeled midline crossing fibers per thousand CST-axons (Fig. 4D), a value only slightly higher than that of normal or lesion only animals.

Plasticity of the corticopontine projection

In all animal groups cortical fibers innervated the basilar pontine nuclei ipsilaterally in a topographic pattern typical for their origin in the forelimb motor cortex (Mihailoff et al., 1978; Wiesendanger and Wiesendanger, 1982; Panto et al., 1995). At rostral levels one dense

termination field was observed in the center of the ipsilateral pons. At midpontine levels the termination field split into three longitudinal columns (medial, intermedial, and lateral column). In addition, dorsomedial and dorsolateral termination zones were present. At caudal levels all these termination zones fused again, and a dense terminal plexus was observed in the medial, intermedial and lateral pons and around the ventral and dorsal aspect of the cerebral peduncle. This ipsilateral projection pattern to the basilar pontine nuclei was similar in all experimental groups with no observable difference in fiber distribution. However, quantification of the ipsilateral projection showed significant differences in the lesioned, mAb IN-1-treated and in the P2-lesioned group: Lesioned, mAb IN-1-treated animals showed an increased innervation index, whereas after neonatal cortical lesions these values were slightly lower than in control rats (see Fig. 6A).

Greater differences among the experimental groups were seen for the contralateral projections. In normal rats and in the control animals (lesion only and lesioned, anti-HRP-treated) only a very minor contralateral projection, restricted to the midpontine, caudal level and to regions close to the midline was found (Figs. 5A,B, 6B). In lesioned, mAb IN-1-treated animals the contralateral pons showed a strong innervation, again mainly at midpontine and caudal pontine levels (Figs. 5C,D, 6B). A very pronounced increase of fibers projecting to the contralateral pons was seen in animals lesioned at P2 (Figs. 5E,F, 6B). The innervation index of the contralateral pons was 0.504 ± 0.126 for normal, 0.593 ± 0.119 for lesion only and 0.679 ± 0.175 for anti-HRP-treated rats, in comparison with 2.106 ± 0.407 for mAb IN-1-treated and 5.845 ± 1.646 for neonatally lesioned animals (Fig. 6B). Relating the contralateral to the ipsilateral innervation index showed a significant increase of that ratio in lesioned, IN-1 antibody treated and P2-lesioned animals (Fig. 6E).

Counting of midline crossing fibers in the pons showed a highly significant increase in lesioned animals receiving mAb IN-1 treatment: 157.4 ± 18.3 fibers per thousand labeled CST axons compared with 23.47 ± 4.56 in anti-HRP-treated animals (Fig. 6C). Figures 5CI and 5DI show these crossing fibers of mAb IN-1-treated animals at midpontine (Fig. 5CI) and caudal pontine level (Fig. 5DI). Neonatally lesioned animals showed a more than 2.5-fold increase of midline crossing fibers (46.95 ± 2.6) compared with lesion only animals (16.86 ± 1.43; Fig. 6C).

To check whether the increased contralateral pontine projection was due to the greater number of midline crossing fibers or an increase of terminal arborization, we related the iODs of the contralateral side to the numbers of midline crossing fibers. Figure 6D shows that the increased labeling in the denervated, contralateral pons in the mAb IN-1-treated rats exactly paralleled the enhanced number of midline crossing fibers. In contrast, neonatally lesioned animals showed a significantly increased contralateral labeling per crossing fiber (Fig. 6D).

Due to the anatomical subdivision of the pontine nuclei and their complex cortical input pattern we analyzed the rostrocaudal distribution of midline crossing fibers and their ipsilateral and contralateral terminations (Figs. 6F, 7A,B). The distribution of the ipsilateral projection to the rostral, intermediate, and caudal part of the pons was similar in all groups: slightly more labeling was found in the caudal part than in the rostral and intermediate part of the pons (Fig.7A). The contralateral projection, however, showed some differences between individual compartments in the P2 group (Fig. 7B): the intermediate pons of the P2-lesioned rats received a smaller, and the caudal pons a larger proportion of cortical axons. The control and mAb IN-1-treated groups were not significantly different. A similar effect was found for the number of crossing fibers in the neonatally lesioned animals, but with a less clear manifestation (Fig. 6F).

To analyze further the topographic specificity of the contralateral pontine innervation the mediolateral distribution of the corticopontine fibers in the intermediate and caudal part of the ipsilateral and contralateral pons was assessed. Figure 8 shows the medio-lateral innervation density profile of a lesioned, anti-HRP, a lesioned, mAb IN-1-treated, and a neonatally lesioned, untreated animal. Whereas the very minor contralateral innervation in the lesioned, control antibody treated rats is restricted to the region close to the midline, the lesioned, mAb IN-1-treated, and neonatally lesioned animals show a symmetrical bilateral innervation pattern in the intermediate pons; in the caudal pons the new, contralateral projection is more restricted in the mediolateral extent than the ipsilateral projection. The histograms show that the new, contralateral innervation of the pontine nuclei is topographically organized and specific for fibers originating in the forelimb motor area.

DISCUSSION

The present results show the occurrence of sprouting and plastic remodeling of corticorubral and corticopontine fibers in the adult brain after neutralization of the myelin-associated neurite growth inhibitors by the monoclonal antibody IN-1. Following removal of one caudal motor cortex, fibers originating in the forelimb area of the intact side crossed over the midline and terminated in the denervated contralateral red nucleus and pons. The anatomical distribution of these sprouted fibers mirrored the normal ipsilateral somatotopic projection. Similar lesion-induced sprouting was found after neonatal cortical lesions.

Increased fiber number in the cerebral peduncle in P2-lesioned rats

Counting of BDA-labeled fibers in the cerebral peduncle revealed no significant differences between the intact, the lesion only, the lesioned, anti-HRP-treated and the lesioned, mAb IN-1-treated groups. Although the injection site (caudal forelimb area of the motor cortex) and the parameters for the iontophoretic injection of BDA did not differ in animals that sustained lesions as neonates, a large, almost threefold increase of labeled fibers in the cerebral peduncle was observed, and the labeling pattern was different: In the P2 group fibers were distributed homogeneously over the cerebral peduncle whereas the other groups showed only little labeling laterally. The increase probably reflects a survival effect—due to the lack of fibers in the contralateral pathway. Target-derived factors from the enlarged target area may have decreased the normally occurring postnatal reduction of CST fibers (Nah et al., 1980; Mihailoff et al., 1984) from the intact hemisphere. This may fit with the observation in earlier studies (Kolb and Tomie, 1988; Kolb et al., 1992) that after early cortical lesions, the remaining hemisphere has an increased thickness of the cortex.

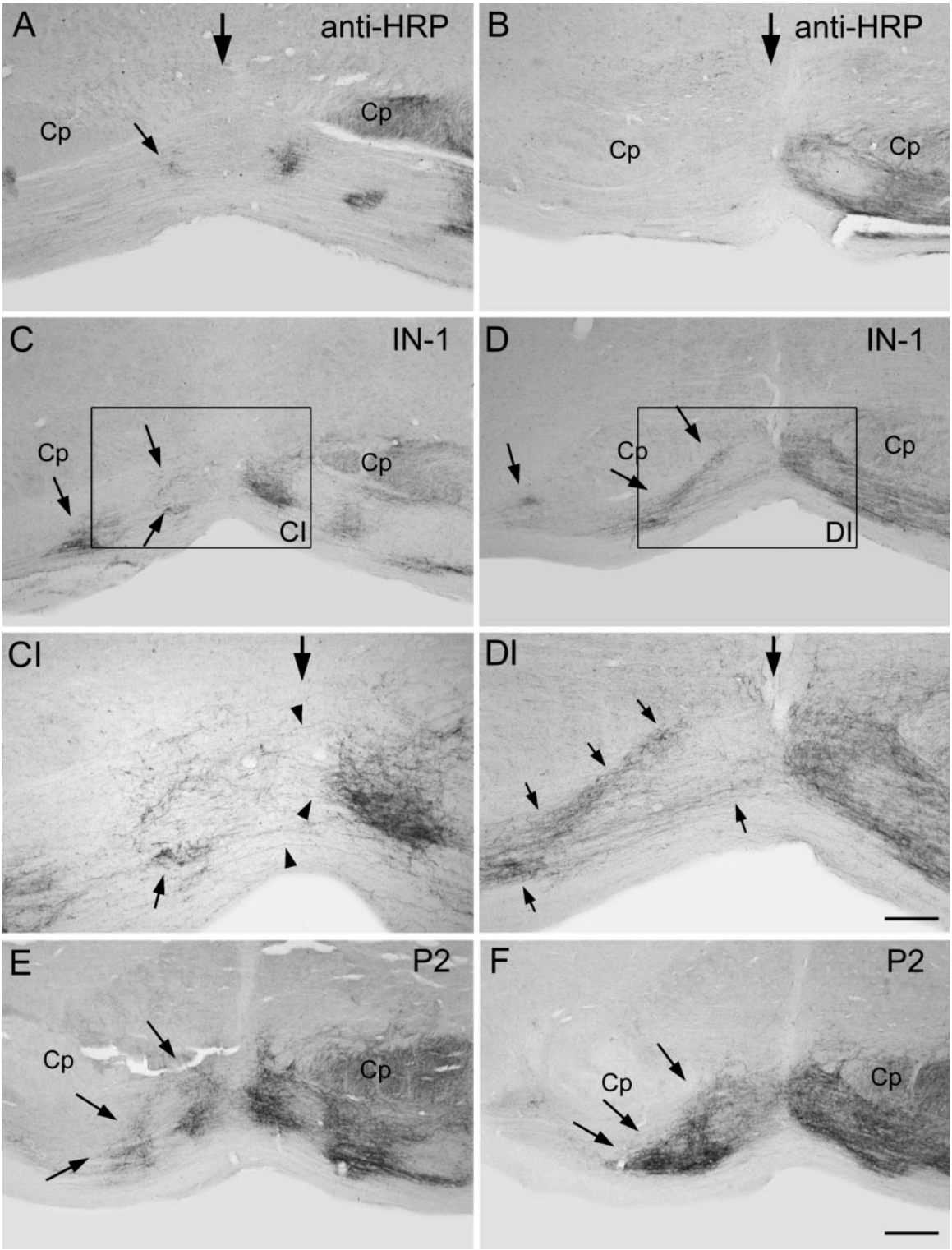

Fig. 5. Cross sections through the basilar pontine nuclei. Photomicrographs on the left side (A, C, CI, E) show the column structure in the intermediate part; those on the right side show sections through the caudal part of the pons (B, D, DI, F). In A–F, large arrows indicate the midline and small arrows the contralateral projection. **A,B:** Animals treated with the antibody anti-HRP show only very few fibers terminating contralaterally (left half of the photographs). Only a small innervation is clearly visible in the medial column of the intermediate part (small arrow, A). **C,D:** Highly increased contralateral projection after two weeks of treatment with the mAb IN-1. The innervation pattern in the denervated pons (left) mirrors the innervation pattern in the intact pons (right), although most of the contralateral projection is found in the medial and intermedial column. **CI:** Higher magnification of the boxed area in **C**, to visualize corticorubral fibers (arrowheads) crossing the midline (large arrow) at midpontine level. **DI:** Higher magnification of the boxed area in **D**, showing the dense termination field (small arrows) in the denervated basilar pontine nuclei of the caudal pons after two weeks of treatment with the mAb IN-1. **E,F:** Sections through the pons in neonatal lesioned animals showed a similar pattern as mAb IN-1-treated rats (ipsi- and contralaterally), but the innervation density is much higher. In these animals, new sprouting was also observed mainly in the medial parts of the denervated side. Scale bars = 320 µm in F (applies to A–F), 160 µm in DI (applies to CI and DI).

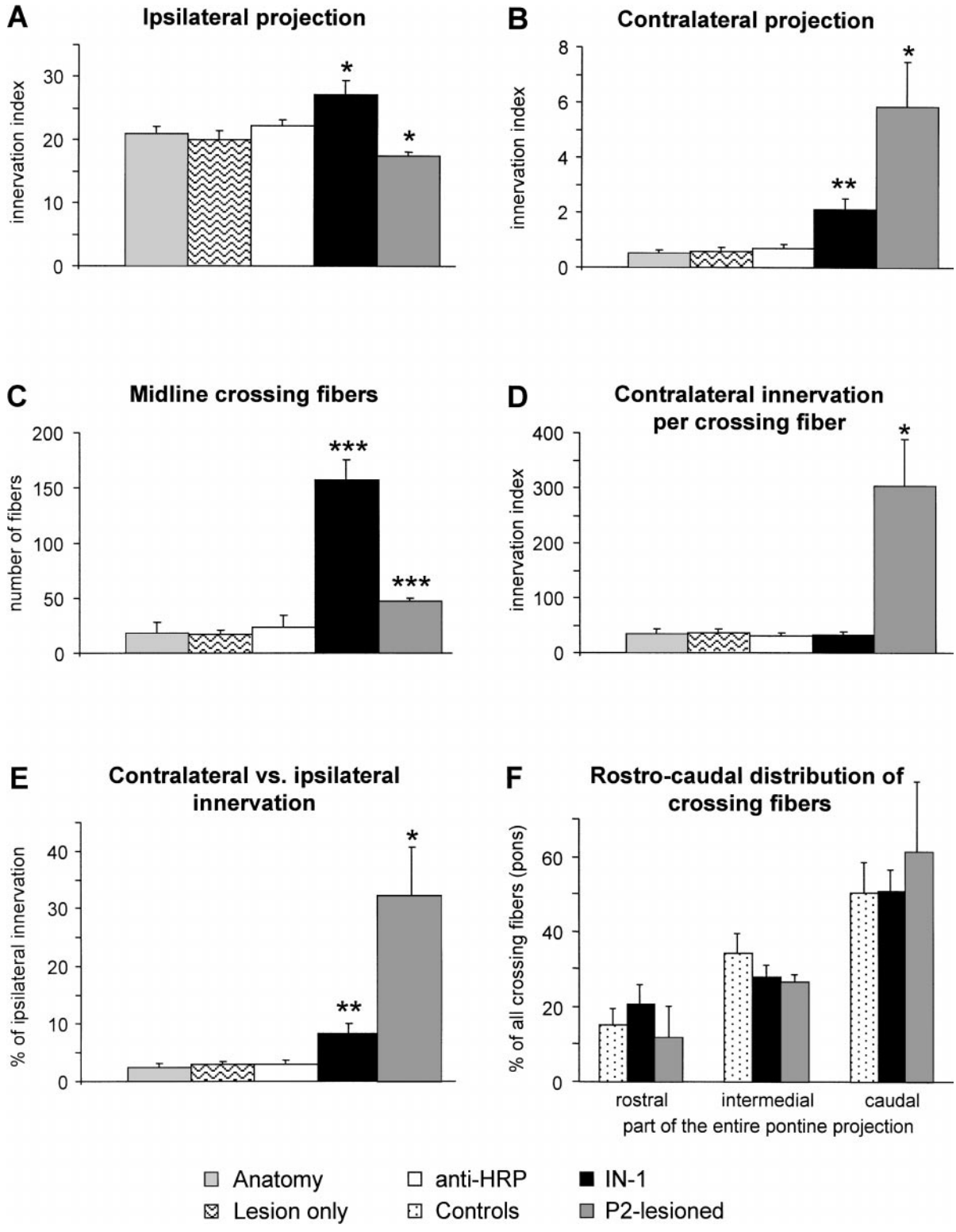

Fig. 6. Quantification of the labeled ipsi- and contralateral pontine projection fields, their innervation pattern, and the midline crossing fibers. **A:** Ipsilateral pontine projection (innervation index = optical density of all ipsilateral termination fields divided by the number of labeled CST-fibers; see Fig. 2C and Materials and Methods). The mAb IN-1-treated animals show a small but significant increase in the ipsilateral innervation index. Neonatally lesioned animals show a small decrease. **B:** Contralateral, denervated side. (Note the different scale of the y-axis compared with A.) The innervation index of the mAb IN-1-treated animals is threefold higher than in control animals; that of neonatally lesioned animals shows a ninefold increase. **C:** Number of pontine midline crossing fibers per thousand labeled CST-axons. In mAb IN-1-treated animals, sixfold more corticopontine fibers cross the midline than in controls, whereas in neonatally lesioned animals twofold more fibers cross the midline. **D:** When the contralateral innervation density is expressed in relation to midline crossing fibers, only neonatally lesioned animals show an increased value. **E:** Ratio of the contralateral to the ipsilateral innervation. **F:** Rostro-caudal distribution of midline crossing fibers in the three main parts of the pons (rostral, intermedial, and caudal part). In each group, most of the crossing fibers are localized in the caudal pons. Controls include anatomy, lesion only, and anti-HRP-treated animals, which show comparable values. Mean values ± SEM. Asterisks indicate significance (IN-1 compared with anti-HRP and P2-lesioned compared with lesion only. Exception: in B and C, P2-lesioned is compared with IN-1); *, $P < 0.05$; **, $P < 0.01$; ***, $P < 0.001$, t-test, two tailed.

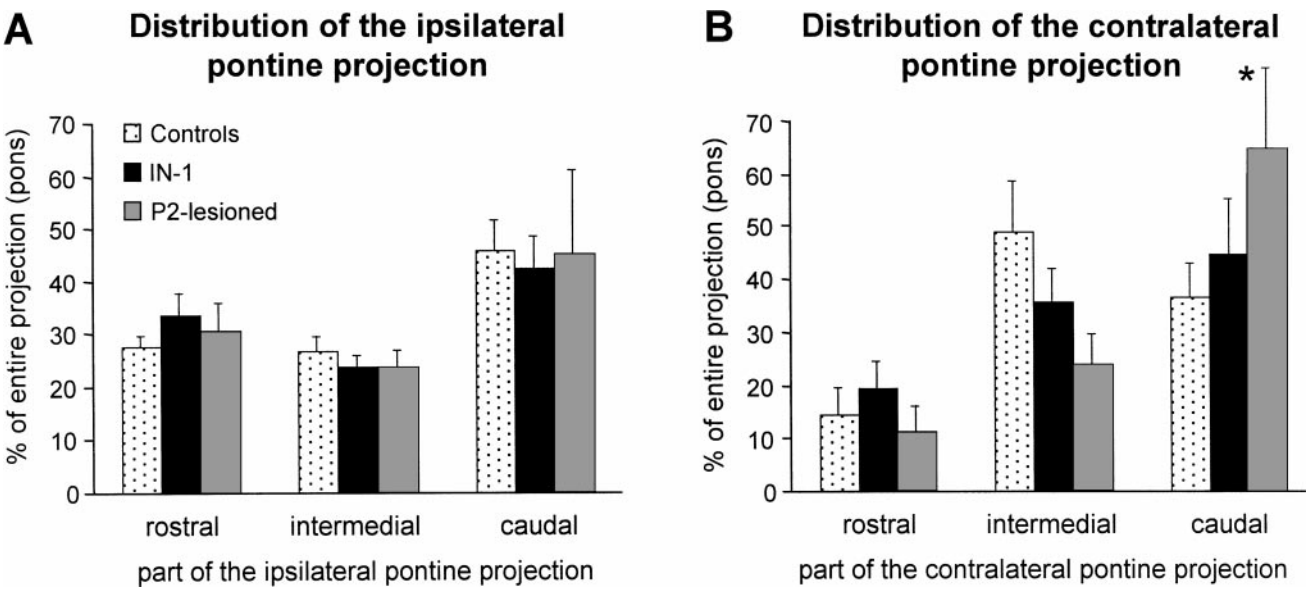

Fig. 7. **A:** The rostro-caudal distribution of the ipsilateral projection to the pontine nuclei does not alter after treatment. About 50% of the ipsilateral labeling is found in the caudal pons in all groups. **B:** On the contralateral side neonatally lesioned animals show a relative increase of this caudal projection. Controls include anatomy, lesion only, and anti-HRP-treated animals. Mean values ± SEM.

Topographic sprouting of corticorubral fibers

Studies of the corticorubral projections in the normal rat reported a predominantly ipsilateral innervation of the parvocellular part of the red nucleus (Brown, 1974; Gwyn and Flumerfelt, 1974; Flumerfelt, 1980; Naus et al., 1985a). Only few fibers crossed the midline and terminated in the contralateral red nucleus (Murakami and Higashi, 1988; Z'Graggen et al., 1998). Our results showed an increase of midline crossing corticorubral fibers originating in the forelimb area of the intact hemisphere after unilateral motor cortex ablation and mAb IN-1 treatment in adult rats. The corticorubral axons reached the contralateral parvocellular red nucleus and formed a dense innervation plexus. Such corticorubral sprouting after motor cortex ablation has so far only been described after neonatal lesions in cats and rats (Leong, 1976; Nah and Leong, 1976; Villablanca et al., 1982; Naus et al., 1985b; Murakami and Higashi, 1988; Fisher et al., 1988). The examination of the rats that underwent the cortical lesion at P2 confirmed these earlier findings. In the P2-lesioned as well as in the lesioned, mAb IN-1-treated adult rats, the crossing fibers terminated in a topographically correct pattern, i.e., in the most rostral, parvocellular part of the red nucleus. The new, contralateral termination mirrored the normal, ipsilateral projection.

Topographic sprouting of corticopontine fibers

In normal rats, forelimb motor corticopontine projections terminate somatotopically within the ipsilateral pontine nuclei. Only very few fibers cross the midline and terminate within the contralateral pontine gray, mostly close to the midline (Mihailoff et al., 1978; Wiesendanger and Wiesendanger, 1982; Castro and Mihailoff, 1983; Kartje-Tillotson et al., 1986). Adult lesioned, mAb IN-1-treated animals showed an increased number of midline crossing fibers and a relatively dense contralateral innervation. The crossed projection formed a termination pattern specific for fibers originating in the forelimb area, mirroring the projections of the ipsilateral side. This finding suggests that positional cues and targeting signals may be present or re-expressed that can be recognized by the sprouting axons. Our findings after neonatal lesions coincide with previous studies (Leong and Lund, 1973; Leong, 1976; Mihailoff and Castro, 1981; Castro and Mihailoff, 1983; Kartje-Tillotson et al., 1986): Unilateral ablation of the motor cortex in P2-lesioned rats also resulted in an enhanced contralateral innervation and an increase of midline crossing fibers compared with normal animals. Mihailoff and Castro (1981) found bouton-like structures after such neonatal lesions in the contralateral pons, suggesting that sprouted corticopontine fibers established synapses. Whether sprouted fibers formed synapses after mAb IN-1 treatment is unclear, although we found terminal-like boutons at some fibers. Electron microscopic examinations should be done to answer this question.

In the mAb IN-1-treated animals, more fibers cross the midline than in the animals lesioned as neonates. In the developing CNS specific factors are expressed at the midline that attract or repulse fibers in order to establish the correct pattern. Whether these guidance cues are still expressed in the mature CNS or whether their re-expression is only triggered by a lesion is not yet clear (e.g., in the visual system lesions induce guidance cues; Wizenmann et al., 1993; Bähr et al., 1996).

Interestingly, in the neonatally lesioned rats the contralateral labeling per crossing fiber is increased in comparison with the control animals. In contrast, the ratio between contralateral labeling and crossing corticopontine fibers is unchanged in lesioned, mAb IN-1-treated rats. These observations suggest that the midline crossing

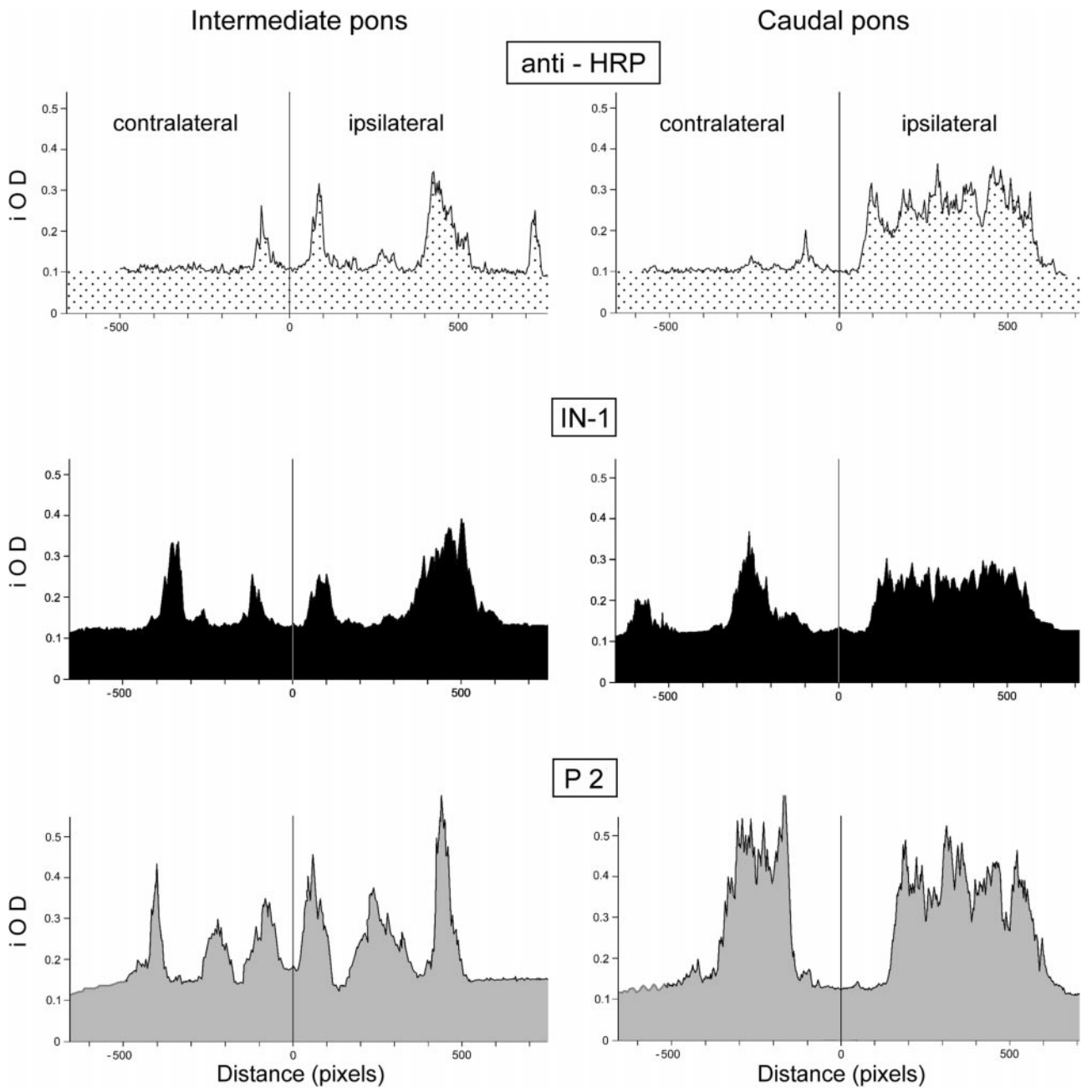

Fig. 8. Density profiles of the mediolateral distribution of the cortical forelimb projection to the basilar pontine nuclei. In both parts, intermediate and caudal pons, the localization of the new contralateral forelimb projection fields (columns) mirrors the ipsilateral projection fields, showing topographic specificity of these crossed projections. 500 pixels = about 900 µm. The OD was measured and integrated over a bar-shaped field (50 × 2300 µm) placed over the areas of the densest labeling on the section, thus resulting in an integrated optical density value.

fibers increase their terminal arborization after neonatal lesions, but not after an adult lesion and mAb IN-1 treatment. This might be due to the different environmental cues in the developing versus the mature CNS. For example, only little or no myelin is present in the pontine nuclei in the neonatally lesioned group at the time of the lesion, whereas in the adult rats myelin is present and only the myelin-associated neurite growth inhibitors (NI-35/250) are neutralized by mAb IN-1. In addition, the P2-lesioned rats had a much longer survival time, one year, compared with the lesioned, mAb IN-1-treated animals that survived only for 14 days.

Interestingly, the ipsilateral corticopontine projection changed in the P2-lesioned and the lesioned, mAb IN-1-treated animals. The ipsilateral innervation index was slightly reduced after neonatal unilateral cortical ablation compared with normal animals. Chemoattractive cues might guide a portion of the corticopontine fibers directly

to the contralateral, denervated pontine nuclei. We observed, however, that the innervation index of the ipsilateral pontine nuclei was increased after lesion and mAb IN-1 treatment in adult rats. The possibility that lesion-induced sprouting leads not only to re-innervation of the contralateral, deafferented pons but also affects the ipsilateral pontine nuclei, which are affected by the loss of the very minor projection from the lesioned hemisphere, seems likely. Other reports support the idea that the application of mAb IN-1 can have an effect on areas other than the ones deafferented by the lesion (e.g., Z'Graggen et al., 1998; G.L. Kartje, personal communication).

Possible mechanisms

After removal of one sensorimotor cortex in neonatal rats, the remaining hemisphere innervates the red nucleus, the pontine nuclei, and the spinal cord bilaterally (Leong and Lund, 1973; Leong, 1976; Nah and Leong, 1976; Mihailoff and Castro, 1981; Villablanca et al., 1982; Castro and Mihailoff, 1983; Naus et al., 1985b; Kartje-Tillotson et al., 1986; Murakami and Higashi, 1988; Kuang and Kalil, 1990). Earlier studies showed that these bilateral connections are not surviving pre-existing, normally transient connections but that they are newly formed as a consequence of the neonatal cortex lesion (Nah et al., 1980; Mihailoff et al., 1984). These findings suggest the induction of factors by target denervation that may induce sprouting and guide the newly grown axons. Neurotrophins or chemoattractants but also extracellular matrix or surface molecules are likely candidates (Thoenen, 1995; Fagan et al., 1997). The role of the very few pre-existing crossing fibers in guiding newly growing fibers is not clear. As we found midline crossing fibers after the lesion preferentially where we found the few, crossing fibers in normal animals, a guidance function of those pre-existing fibers is possible. In the case of neonatally lesioned rats, Naus and colleagues used two retrograde tracers to determine whether the crossing fibers in the red nucleus following neonatal lesions are collaterals of the ipsilaterally projecting fibers. They did not find any double-labeled cortical neurons, suggesting that at least after neonatal cortical lesions the new, contralateral corticorubral projection does not consist of collaterals of the normal innervation (Naus et al., 1986). In contrast, Murakami and Higashi (1988) found in the cat that individual corticorubral neurons project bilaterally in normal development and following unilateral cortical lesions. In the present study midline crossing axons with branches and terminal arbors on both sides of the midline were frequently observed. The suggestion that most of these crossing fibers are collaterals from preexisting, ipsilaterally projecting corticorubral axons is supported by the unchanged fiber number in the cerebral peduncle in all adult lesioned groups. This is in contrast to the situation after P2 lesions, where the number of corticofugal axons was increased and, in parallel and at almost the same proportion, the number of crossing corticorubral axons.

In the pons the ratio of the fiber density in the termination area to the number of midline crossing axons (not increased in mAb IN-1-treated rats; greatly increased in P2-lesioned animals) indicates that a large relative increase in terminal arborization mainly occurs in the newborn animals after a lesion. In contrast, in the animals lesioned as adults, the contralateral pontine innervation is mainly due to an increased number of midline crossing corticopontine axons or axon collaterals.

The myelin-associated neurite growth inhibitors (IN-1 antigens) probably influence plasticity after adult CNS lesions

After unilateral cortical ablation and treatment with mAb IN-1, we could demonstrate structural plasticity that is normally restricted to a short postnatal period. In earlier studies corticorubral sprouting occurred only after lesions up to 17 days of age, and corticopontine sprouting was never observed when lesions were made at 20 days of age (Leong, 1976). However, lesion-induced sprouting can take place well after this developmental period if a growth-permissive environment is created by applying the neutralizing antibody IN-1. Whether the mAb IN-1 treatment has functional benefits in this lesion paradigm is currently under investigation.

Clinical considerations and conclusions

Human CNS myelin was shown to contain inhibitory proteins with similar biochemical properties and comparable high molecular weight (200–300 kD) as bovine (bNI-220; Spillmann et al., 1998) and rat material (NI-35/250; Spillmann et al., 1997). The rat monoclonal antibody IN-1 was able to neutralize the human CNS myelin inhibitory property in vitro (Spillmann et al., 1997). Taking into account that mAb IN-1 directed against rat NI-250 could also neutralize the inhibitory activity of frog, opossum, and bovine CNS myelin (Lang et al., 1995; Varga et al., 1995; Spillmann et al., 1998), it is very likely that the IN-1 antigen is highly conserved among different species. A well-established observation is that the outcome of a CNS lesion in humans also depends on the age at which the lesion occurred (Kennard, 1936, 1938). A similar approach might therefore be useful to improve the functional outcome after brain lesions in humans. New tools like humanized IN-1 Fab fragments are currently becoming available (Bandtlow et al., 1996; Brösamle et al., 1996).

In conclusion, our results indicated that new, crossed corticofugal projections form and innervate somatotopically the pons and red nucleus following unilateral motor cortex lesion and mAb IN-1 treatment. Neutralization of the myelin-associated neurite growth inhibitors might therefore be a promising tool to improve the functional recovery of patients after CNS lesions.

ACKNOWLEDGMENTS

The authors acknowledge Werner Z'Graggen and Joachim Tönnes for valuable discussions, Roland Schöb for photographic support, and Eva Hochreutener for help with the graphics. We thank Regula Schneider for help with the histology, Barbara Niederöst for supporting us with hybridoma cells, and Johanna Höhn and Denise Nierentz for their skilful care of the rats.

REFERENCES

Bähr M, Wizenmann A. 1996. Retinal ganglion cell axons recognize specific guidance cues present in the deafferented adult rat superior colliculus. J Neurosci 16:5106–5116.

Bandtlow C, Zachleder T, Schwab ME. 1990. Oligodendrocytes arrest neurite growth by contact inhibition. J Neurosci 10:3837–3848.

Bandtlow C, Schiweck W, Tai HH, Schwab ME, Skerra A. 1996. The *Escherichia coli*-derived Fab fragment of the IgM/kappa antibody IN-1 recognizes and neutralizes myelin-associated inhibitors of neurite growth. Eur J Biochem 241:468–475.

Barth TM, Stanfield BB. 1990. The recovery of forelimb-placing behavior in rats with neonatal unilateral cortical damage involves the remaining hemisphere. J Neurosci 10:3449–3459.

Brandt HM, Apkarian AV. 1992. Biotin-dextran: a sensitive anterograde tracer for neuroanatomic studies in rat and monkey. J Neurosci Methods 45:35–40.

Bregman BS, Kunkel-Bagden E, Schnell L, Dai HN, Gao D, Schwab ME. 1995. Recovery from spinal cord injury mediated by antibodies to neurite growth inhibitors. Nature 378:498–501.

Brösamle C, Schnell L, Skerra A, Schwab ME. 1996. A recombinant Fab fragment against myelin associated neurite growth inhibitors promotes axonal regeneration of lesioned corticospinal fibers in the adult rat. Soc Neurosci Abs 130:2.

Brown LT. 1974. Corticorubral projections in the rat. J Comp Neurol 154:149–167.

Caroni P, Schwab ME. 1988a. Two membrane protein fractions from rat central myelin with inhibitory properties for neurite growth and fibroblast spreading. J Cell Biol 106:1281–1288.

Caroni P, Schwab ME. 1988b. Antibody against myelin-associated inhibitor of neurite growth neutralizes nonpermissive substrate properties of CNS white matter. Neuron 1:85–96.

Castro AJ. 1975. Ipsilateral corticospinal projections after large lesions of the cerebral hemisphere in neonatal rats. Exp Neurol 46:1–8.

Castro AJ, Mihailoff GA. 1983. Corticopontine remodelling after cortical and/or cerebellar lesions in newborn rats. J Comp Neurol 219:112–123.

Fagan AM, Suhr ST, Lucidi-Phillipi CA, Peterson DA, Holtzman DM, Gage FH. 1997. Endogenous FGF-2 is important for cholinergic sprouting in the denervated hippocampus. J Neurosci 17:2499–2511.

Fisher RS, Sutton RL, Hovda DA, Villablanca JR. 1988. Corticorubral connections: ultrastructural evidence for homotypic synaptic reinnervation after developmental deafferentiation. J Neurosci Res 21:438–446.

Flumerfelt BA. 1980. An ultrastructural investigation of afferent connections of the red nucleus in the rat. J Anat 131:621–633.

Gomez-Pinilla F, Villablanca JR, Sonnier BJ, Levine MS. 1986. Reorganization of pericruciate cortical projections to the spinal cord and dorsal column nuclei after neonatal or adult cerebral hemispherectomy in cats. Brain Res 385:343–355.

Graybiel AM, Devor M. 1974. A microelectrophoretic delivery technique for use with horseradish peroxidase. Brain Res 68:130–135.

Gwyn DG, Flumerfelt BA. 1974. A comparison of the distribution of cortical and cerebellar afferents in the red nucleus of the rat. Brain Res 69:130–135.

Herzog A, Brösamle C. 1997. Semifree-floating treatment—a simple and fast method to process consecutive sections for immunohistochemistry and neuronal tracing. J Neurosci Methods 72:57–63.

Hicks SP, D'Amato CJ. 1970. Motor-sensory and visual behavior after hemispherectomy in newborn and mature rats. Exp Neurol 29:416–438.

Kapfhammer JP, Schwab ME. 1994. Inverse patterns of myelination and GAP-43 expression in the adult CNS: neurite growth inhibitors as regulators of neuronal plasticity? J Comp Neurol 340:194–206.

Kartje-Tillotson G, Neafsey EJ, Castro AJ. 1985. Electrophysiological analysis of motor cortical plasticity after cortical lesions in newborn rats. Brain Res 332:103–111.

Kartje-Tillotson G, Neafsey EJ, Castro AJ. 1986. Topography of corticopontine remodelling after cortical lesions in newborn rats. J Comp Neurol 250:206–214.

Kartje-Tillotson G, Donoghue DL, Dauzvardis MF, Castro AJ. 1987. Pyramidotomy abolished the abnormal movements evoked by intracortical microstimulation in adult rats that sustained neonatal cortical lesions. Brain Res 415:172–177.

Kennard MA. 1936. Age and other factors in motor recovery from precentral lesions in monkeys. Am J Physiol 115:138–146.

Kennard MA. 1938. Reorganization of motor function in the cerebral cortex of monkeys deprived of motor and premotor areas in infancy. J Neurophysiol 1:477–496.

Kolb B, Tomie JA. 1988. Recovery from early cortical damage in rats. IV. Effects of hemidecortication at 1, 5, or 10 days of age on cerebral anatomy and behavior. Behav Brain Res 28:259–274.

Kolb B, Whishaw IQ. 1989. Plasticity in the neocortex: mechanisms underlying recovery from early brain damage. Prog Neurobiol 32:235–276.

Kolb B, Gibb R, van der Kooy D. 1992. Cortical and striatal structure and connectivity are altered by neonatal hemidecortication in rats. J Comp Neurol 322:311–324.

Kosinski RJ, Neafsey EJ, Castro AJ. 1986. A comparative topographical analysis of dorsal column nuclear and cerebral cortical projections to the basilar pontine gray in rats. J Comp Neurol 244:163–173.

Kuang RZ, Kalil K. 1990. Specificity of corticospinal axon arbors sprouting into denervated contralateral spinal cord. J Comp Neurol 302:461–472.

Lang DM, Rubin BP, Schwab ME, Stürmer CAO. 1995. CNS myelin oligodendrocytes of the *Xenopus* spinal cord—but not optic nerve—are nonpermissive for axon growth. J Neurosci 15:99–109.

Leong SK. 1976. An experimental study of the corticofugal system following cerebral lesions in the albino rat. Exp Brain Res 26:235–247.

Leong SK, Lund RD. 1973. Anomalous bilateral corticofugal pathways in albino rats after neonatal lesions. Brain Res 62:218–221.

Mihailoff GA, Castro AJ. 1981. Autoradiographic and electron microscopic degeneration evidence for axonal sprouting in the rat corticopontine system. Neurosci Lett 21:267–273.

Mihailoff GA, Burne RA, Woodward DJ. 1978. Projections of the sensorimotor cortex to the basilar pontine nuclei in the rat: an autoradiographic study. Brain Res 145:347–354.

Mihailoff GA, Adams CE, Woodward DJ. 1984. An autoradiographic study of the postnatal development of sensorimotor and visual components of the corticopontine system. J Comp Neurol 222:116–127.

Murakami F, Higashi S. 1988. Presence of crossed corticorubral fibers and increase of crossed projections after unilateral lesions of the cerebral cortex of the kitten: a demonstration using anterograde transport of *Phaseolus vulgaris* leucoagglutinin. Brain Res 447:98–108.

Nah SH, Leong SK. 1976. Bilateral corticofugal projection to the red nucleus after neonatal lesions in the albino rat. Brain Res 107:433–436.

Nah SH, Ong LS, Leong SK. 1980. Is sprouting the result of a persistent neonatal connection? Neurosci Lett 19:39–44.

Naus CG, Flumerfelt BA, Hrycyshyn AW. 1985a. An HRP-TMB ultrastructural study of rubral afferents in the rat. J Comp Neurol 239:453–465.

Naus CG, Flumerfelt BA, Hrycyshyn AW. 1985b. An anterograde HRP-WGA study of aberrant corticorubral projections following neonatal lesions of rat sensorimotor cortex. Exp Brain Res 59:365–371.

Naus CG, Flumerfelt BA, Hrycyshyn AW. 1986. Contralateral corticorubral fibers induced by neonatal lesions are not collaterals of the normal ipsilateral projection. Neurosci Lett 70:52–58.

Neafsey EJ, Bold EL, Haas G, Hurley-Gius KM, Quirk G, Sievert CF, Terreberry RR. 1986. The organization of the rat motor cortex: a microstimulation mapping study. Brain Res 396:77–96.

Panto MR, Cicirata F, Angaut P, Parenti R, Serapide F. 1995. The projection from the primary motor and somatic sensory cortex to the basilar pontine nuclei. A detailed electrophysiological and anatomical study in the rat. J Hirnforsch 36:7–19.

Paxinos G, Watson C. 1982. The rat brain in stereotaxic coordinates. Sydney: Academic Press.

Schnell L, Schwab ME. 1990. Axonal regeneration in the rat spinal cord produced by an antibody against myelin-associated neurite growth inhibitors. Nature 343:269–272.

Schnell L, Schwab ME. 1993. Sprouting and regeneration of lesioned corticospinal tract fibres in the adult rat spinal cord. Eur J Neurosci 5:1156–1171.

Schnell L, Schneider R, Kolbeck R, Barde YA, Schwab ME. 1994. Neurotrophin-3 enhances sprouting of corticospinal tract during development and after adult spinal cord lesion. Nature 367:170–173.

Spillmann AA, Amberger VR, Schwab ME. 1997. High molecular weight protein of human central nervous system myelin inhibits neurite outgrowth: an effect which can be neutralized by the monoclonal antibody IN-1. Eur J Neurosci 9:549–555.

Spillmann AA, Bandtlow CE, Lottspeich F, Keller F, Schwab ME. 1998. Identification and characterization of a bovine neurite growth inhibitor (bNI-220). J Biol Chem 273:19283–19293.

Thallmair M, Metz GAS, Z'Graggen WJ, Raineteau O, Kartje GL, Schwab ME. 1998. Neurite growth inhibitors restrict plasticity and functional recovery following corticospinal tract lesions. Nature Neurosci 1:124–131.

Thoenen H. 1995. Neurotrophins and neuronal plasticity. Science 270:593–598.

Varga ZM, Schwab ME, Nicholls JG. 1995. Myelin-associated neurite growth inhibitory proteins and suppression of regeneration of immature spinal cord in culture. Proc Natl Acad Sci USA 92:10959–10963.

Veenman CL, Reiner A, Honig MG. 1992. Biotinylated dextran amine as an anterograde tracer for single-and double-labeling studies. J Neurosci Methods 41:239–254.

Villablanca JR,Olmstead CE, Sonnier BJ, McAllister I, Gomez F. 1982. Evidence for a crossed corticorubral projection in cats with one cerebral hemisphere removed neonatally. Neurosci Lett 33:241–246.

Whishaw IQ, Kolb B. 1988. Sparing of skilled forelimb reaching and corticospinal projections after neonatal motor cortex removal or hemidecortication in the rat: support for the Kennard doctrine. Brain Res 451:97–114.

Wiesendanger R, Wiesendanger M. 1982. The corticopontine system in the rat. II. The projection pattern. J Comp Neurol 208:227–238.

Wizenmann A, Thies E, Klostermann S, Bonhoeffer F, Bähr M. 1993. Appearance of target-specific guidance information for regenerating axons after CNS lesions. Neuron 11:975–983.

Z'Graggen WJ, Metz GAS, Kartje GL, Thallmair M, Schwab ME. 1998. Functional recovery and enhanced corticofugal plasticity after unilateral pyramidal tract lesion and blockade of myelin-associated neurite growth inhibitors in adult rats. J Neurosci 18:4744–4757.